A Quantum Mechanical Investigation of the Crystal and Electronic Structures of Solid Solutions of Pyrite-type Dipnictides MPn_2 (M = Si, Ge, Ni, Pd, Pt)

F. Bachhuber[a,b], J. Rothballer[b], T. Söhnel[a] and R.Weihrich[b]

[a] *School of Chemical Sciences, The University of Auckland, New Zealand.*
[b] *Institute of Inorganic Chemistry, The University of Regensburg, Germany*

Solid solutions of pyrite-type dipnictides MPn_2 (M = Si, Ge, Ni, Pd, Pt) are studied by DFT calculations with an emphasis on different ordering variants. The compounds are analyzed in terms of stability to provide opportunity to synthesize novel compounds. The solid solutions are also examined for Vegard behavior and their electronic structures are analyzed.

1. Introduction

There is a large variety of structure types for MPn_2 (Pn = N, P, As, Sb, Bi) compounds with promising properties. Among these structures, a dumbbell-like arrangement of the pnictide atoms is very common. The pyrite-type SiP_2 served as a model compound for DFT calculations on electronic structure in both direct and momentum space as well as IR- and Raman spectra [1,2]. The calculations were extended to the system $SiP_{2-x}As_x$ where P was successively substituted by As [3]. For SiPAs, an ordering scheme derived from the pyrite structure type according to [4] resulted in hetero- and homoatomic dumbbells with the first clearly preferred over the latter due to dipole momentums from the charges of P (-0.8 e) und As (-0.3 e). There are three different ordering variants for the heteroatomic configuration that slightly differ in stability (by a few kJ/mol).

Here we present a systematic approach on pyrite-type MPn_2 and related $MPn1Pn2$ compounds for M = Si, Ge, Ni, Pd, Pt with a special focus on the ordering of the mixed dipnictide compounds. In addition, solid solutions were modeled and examined for Vegard behavior. Electronic stabilities were calculated particularly for the different ordering variants of the compounds with a 1:1:1 stoichiometry. Band structure plots are given to illustrate the electronic structures. Finally, preferences and tendencies within the groups of the periodic table can be derived and conclusions can be drawn on possible new compounds which should be experimentally accessible.

2. Computational details

All total energy calculations were carried out with the full potential local orbital method as implemented in the FPLO program package (version 9.00-34) [5]. The local density approximation (LDA) was used with parametrizations according to Perdew-Wang [6].

3. Results

3.1 Pyrite-type MPn_2 and related ordering variants

The mineral pyrite (FeS_2) crystallizes in the space group (SG) $Pa\bar{3}$ 205 and a unit cell is displayed in Fig. 1(a). The structure can be easily derived from the rock salt structure with Fe (M) atoms forming an *fcc* partial structure (crystallographic position 4a). Instead of single-atom anions, S (Pn) dumbbells are located in the Fe_6 (M_6) octahedral vacancies, resulting in four formula units of FeS_2 (MPn_2) per unit cell. With the Fe (M) atoms on sites 8c, a coordination of S (Pn) atoms by 3 Fe (M) and 1 S (Pn) neighbor is realized that is reminiscent

Fig.1. Structure of mineral pyrite FeS_2
(a) The distorted octahedral coordination of
Fe (*M*) is pointed out as well as the distorted
tetrahedral coordination of S (*Pn*). (b) Structural
fragment of the coordination of an Fe_2 (*M$_2$*) dumbbell.
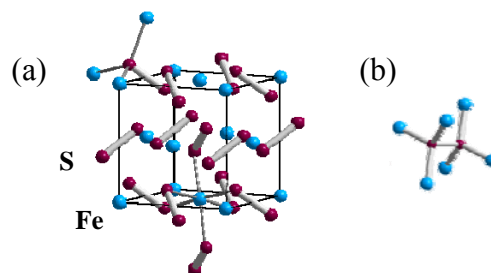
of carbon in an ethane molecule (Fig. 1(b)).

Substituting half of the pnictide dumbbell atoms by a different pnictide atom, four ordering variants can be derived as subgroups of the pyrite structure. Amongst these, there are 3 ordering variants containing heteroatomic *Pn1-Pn2* entities, the ullmannite (cubic, NiSbS, *P2$_1$3*, SG 198, Fig. 2(a)), the cobaltite (orthorhombic, CoAsS, *Pca2$_1$*, SG 29, Fig. 2(b)), and a rhombohedral structure type (*R3*, SG 146, Fig. 2(c)). They differ from each other only in terms of the relative orientation of dumbbells in the unit cell. The fourth ordering variant contains homoatomic dumbbells (monoclinic, *P2$_1$/c*, SG 14, Fig. 2(d)).
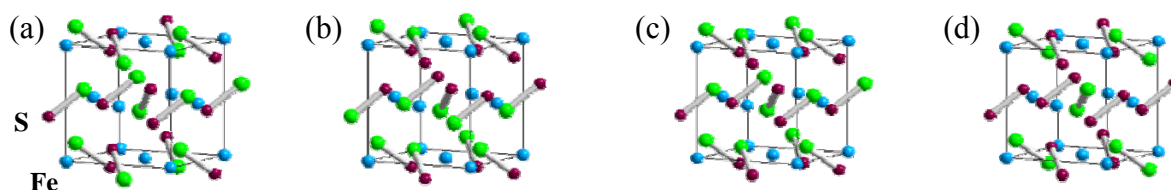

Fig. 2. Ordering variants of mixed dipnictide compounds with a 1:1:1 stoichiometry derived from the pyrite structure. From left to right: (a) *P2$_1$3* (SG 198), (b) *Pca2$_1$* (SG 29), (c) *R3* (SG 146), and (d) *P2$_1$/c* (SG 14).

3.2   Stabilities of pyrite type *MPn$_2$* compounds and related ordering variants *MPn1Pn2*

To determine the stabilities of the investigated compounds, the calculated energy values were compared to the energy values of individual elements in their most stable modifications (α-N_2, orthorhombic (black) P, trigonal (grey) As and Sb, rhombohedral Bi). Fig. 3 shows the calculated stabilities of the compounds *M*N_2, *M*P_2, *M*As_2, *M*Sb_2, and *M*Bi_2 in the pyrite-type structure (SG 205) as well as the compounds *M*NP, *M*PAs, *M*AsSb, and *M*SbBi in SGs 198, 164, 29, and 14, respectively. Negative energies refer to electronic stability.

GeN_2 is the only stable species within the range of the investigated Ge compounds. Not yet synthesized SiN_2 shows the highest electronic stability of all compounds and offers a challenge to experimentalists. Other than that mentioned, compounds with the composition *M*P_2 are most stable and the stability continuously decreases towards *M*Bi_2. As expected, especially Ni, Pd, and Pt compounds follow similar trends. Different energy values in case of several *MPn1Pn2* compositions correspond to different stabilities of the ordering variants. The least stable configuration always refers to the occurrence of homoatomic dumbbells as only present in space group 14. This is also highlighted with the aid of energy-volume diagrams for all 4 ordering variants for the example of SiPAs (framed in yellow, Fig.3). There is a significant energy gap between the configurations with homoatomic dumbbells compared to the configuration with heteroatomic entities. The difference is crucial in terms of stability in case of *M*NP. For *M*AsSb, the energy difference of approximately 20 kJ/mol for *M* = Ni, Pd, Pt indicates an explicit disfavor of SG 14 (all ordering variants are clearly instable for *M* = Si, Ge). The homoatomic configuration is still disfavored by a few kJ/mol for *M*PAs and *M*SbBi. The exact energy values can be found in Table 1.
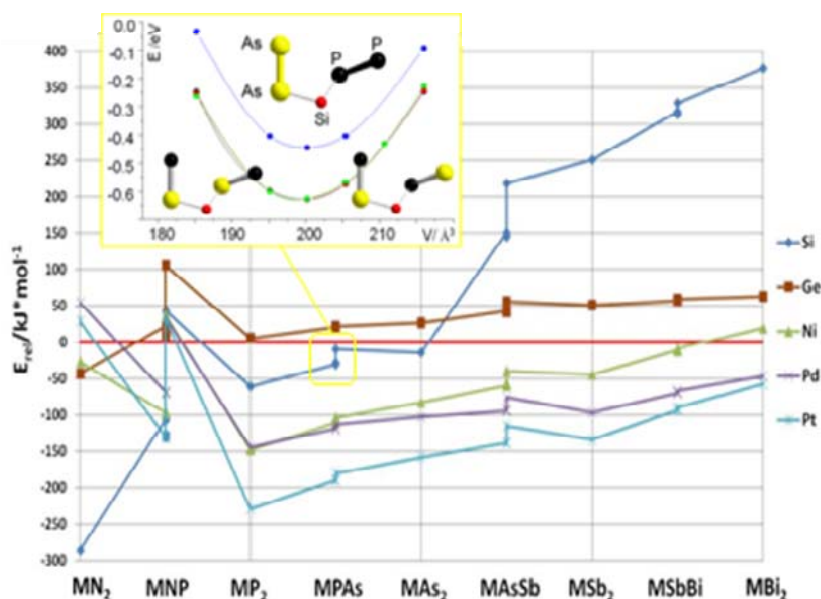
Fig. 3. Relative electronic stabilities of pyrite-type MPn_2 and related $MPn1Pn2$ compounds (M = Si, Ge, Ni, Pd, Pt; Pn = N,P,As,Sb,Bi). An energy-volume plot comparing homo- and heteroatomic dumbbell arrangements is given for SiPAs.

Table 1. Stabilities of pyrite-type MPn_2 and related $MPn1Pn2$ compounds in relation to the electronic energies of the elements. The most stable ordering variants for $MPn1Pn2$ are highlighted in yellow.

MPn2	Si	Ge	Ni	Pd	Pt
N	-286.04	-43.56	-27.37	54.10	28.70
N-P 198	-107.35	21.05	-96.61	-68.23	-129.13
N-P 146	-127.60	10.14	-98.26	-69.89	-131.22
N-P 29	-131.48	8.51	-98.39	-70.34	-131.68
N-P 14	44.06	105.33	37.44	33.88	33.38
P	-61.40	4.79	-148.61	-144.21	-229.73
P-As 198	-30.22	20.27	-110.73	-118.56	-190.23
P-As 146	-28.18	20.14	-111.01	-118.69	-190.04
P-As 29	-30.27	20.06	-110.77	-118.65	-189.71
P-As 14	-10.15	21.84	-104.47	-113.07	-181.30
As	-13.92	25.70	-83.21	-102.51	-158.53
As-Sb 198	151.03	42.25	-59.95	-94.68	-139.47
As-Sb 146	145.74	41.32	-57.05	-93.75	-138.67
As-Sb 29	144.71	41.62	-56.48	-93.41	-138.36
As-Sb 14	218.06	55.57	-39.58	-76.28	-116.20
Sb	250.10	50.41	-45.18	-96.87	-133.67
Sb-Bi 198	316.72	56.49	-11.54	-70.24	-93.38
Sb-Bi 146	313.64	56.09	-11.88	-70.37	-93.66
Sb-Bi 29	312.94	55.97	-11.75	-70.36	-93.64
Sb-Bi 14	328.37	58.51	-8.26	-67.27	-89.49
Bi	376.26	61.96	18.94	-47.18	-57.30

In contrast to the energy differences between the homo- and heteroatomic configurations that can be observed in the plots and the energy-volume curves in Fig. 3, the differences between the 3 ordering variants with a heteroatomic arrangement are too small to be visible. The values are given in Table 1 with the most stable configuration highlighted in yellow. A general preference for SG 29 can be derived for MPN in addition to a preference

for SG 146 for MSbBi and SG 198 for MAsSb with M = Ni, Pd, Pt. The energy differences of the latter range at about 1 kJ/mol and, moreover, they hint towards the existence of ordered structures accessible to experiment. Energy differences of less than 1 kJ/mol should be "taken with a pinch of salt' as they might be within the margin of error.

3.3 Solid solutions of pyrite type MPn_2

Apart from stability considerations, solid solutions of the dipnictide compounds were calculated and examined for Vegard behavior. The volumes of the investigated structures are thus plotted against their Pn content and checked for linear relations (Fig. 4). Except for the range from MN$_2$ to MNP, the curves for Pd and Pt run almost congruently and only the one for Pt is visible in the figure. Between MN$_2$ and MP$_2$, there is no Vegard behavior as the size of the unit cell is determined mainly by the *fcc* metal sublattice with high N content. With a rising P contribution, the dumbbells contribute increasingly to the size of the unit cell. This becomes evident by looking at the significant volume difference between the homo- and heteroatomic arrangement for MNP. On the other hand, Vegard behavior is found for all compounds from the compositions MP$_2$ to MBi$_2$ and similar tendencies of volume changes can be observed. The occurrence of small deviations concerning $MPn1Pn2$ compounds is related to slightly differing lattice constants for homo- and heteroatomic compositions. These deviations are particularly distinctive for MAsSb in accordance with the relatively high energy differences.
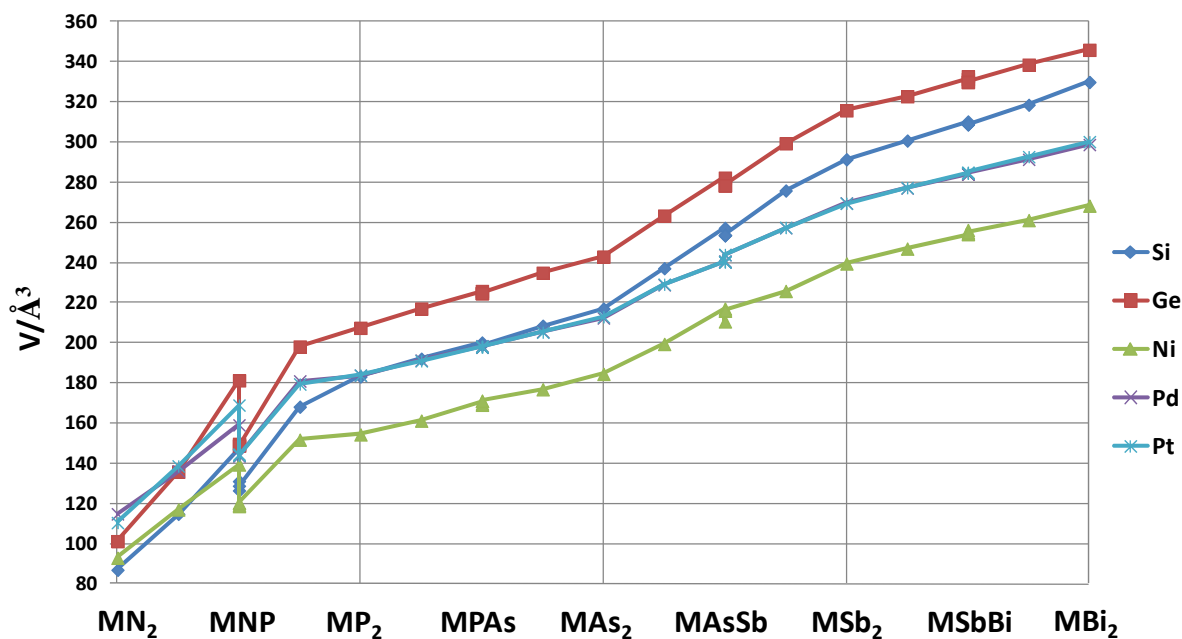

Fig. 4. Volume plots of pyrite-type MPn_2 and related $MPn1Pn2$
compounds (M = Si, Ge, Ni, Pd, Pt; Pn = N,P,As,Sb,Bi) against their Pn content.

3.4 Band structures of pyrite type MN$_2$, MNP, and MP$_2$ (M = Ni, Pd, Pt)

The band structures are given in Fig. 5. The displayed band plots for M = Ni show the metallic character of NiN$_2$ and NiP$_2$ whereas NiNP is a semiconductor. For M = Pd, the same tendency can be found except for PdP$_2$ still being semiconducting. With a very low indirect band overlap and a flat band segment at the Fermi level, PdN$_2$ could exhibit some interesting properties like superconductivity. All compounds with M = Pt are semiconducting and the gap closes towards heavier pnictogen homologues. For all compounds, the gap opens up from Ni to Pt.
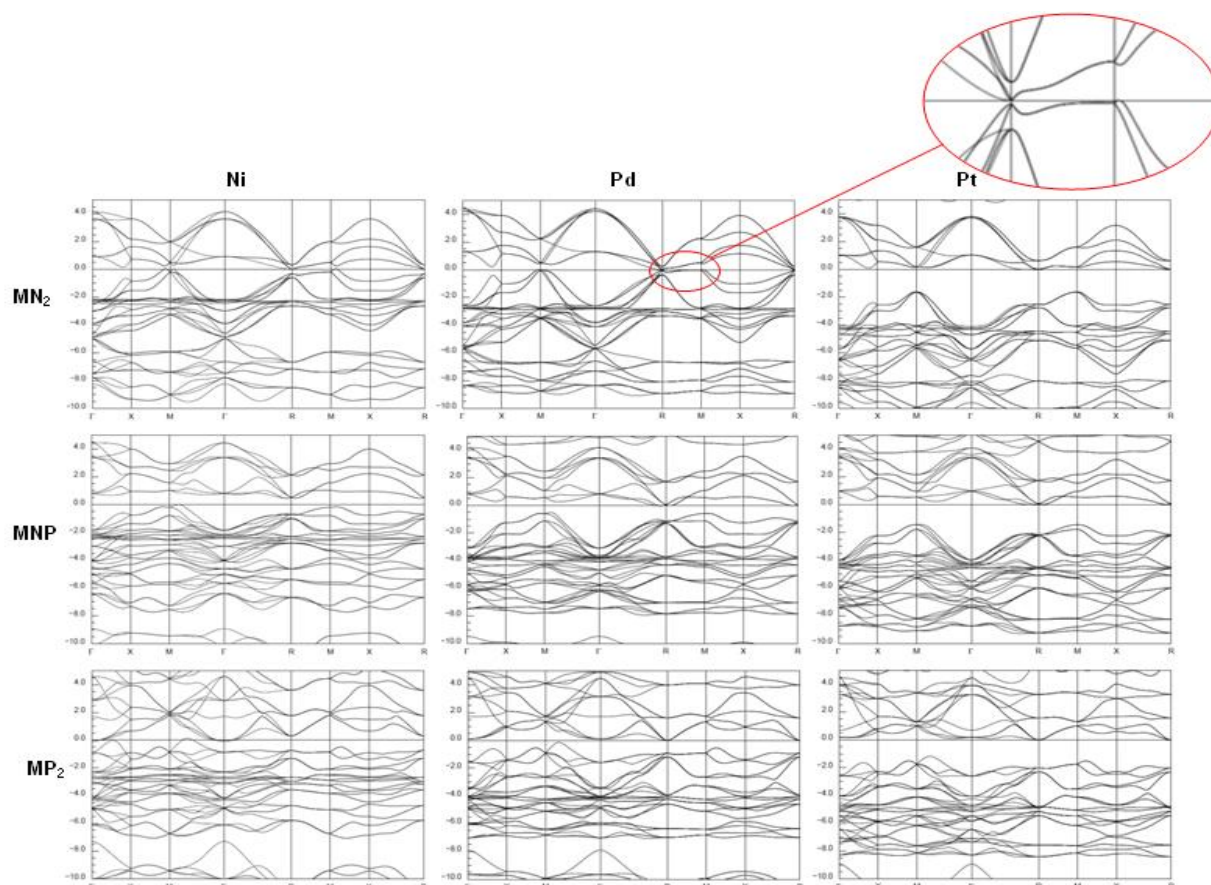
Fig. 5. Band structure plots of pyrite type MN_2, MNP, and MP_2 (M = Ni, Pd, Pt).

4.   Conclusion

In the present work, the crystal and electronic structures of solid solutions of pyrite-type dipnictides MPn_2 (M = Si, Ge, Ni, Pd, Pt) were investigated. Among the compounds with a 1:1:1 stoichiometry, 4 different ordering variants could be derived with a clear energetic preference for an arrangement with heteroatomic dumbbells. The solid solutions show Vegard behavior except for the range between MN_2 and MP_2 and metal to insulator transitions can be seen from the band structures. According to the calculations, some novel compounds with promising properties should be experimentally accessible.

Acknowledgments

References

[1]   Bachhuber F, Rothballer J and Weihrich R 2011 *J. Chem. Phys.* **135** 124508
[2]   Meier M and Weihrich R 2008 *Chem. Phys. Lett.* **461** 38
[3]   Bachhuber F, Rothballer J and Weihrich R 2010 *Z. Anorg. Allg. Chem.* **636** 2116
[4]   Weihrich R et al. 2004 *J. Solid State Chem.* **177** 2591
[5]   Koepernik K and Eschrig H 1999 *Phys. Rev. B* **59** 1743
[6]   Perdew J and Wang Y 1992 *Phys. Rev. B* **45** 13244